

Free vibration analysis of bidirectional functionally graded annular plates resting on elastic foundations using differential quadrature method

Vahid Tahouneh*

Department of Mechanical Engineering, Islamshahr Branch, Islamic Azad University, Tehran, Iran

(Received December 1, 2013, Revised March 22, 2014, Accepted April 3, 2014)

Abstract. This paper deals with free vibration analysis of bidirectional functionally graded annular plates resting on a two-parameter elastic foundation. The formulations are based on the three-dimensional elasticity theory. This study presents a novel 2-D six-parameter power-law distribution for ceramic volume fraction of 2-D functionally graded materials that gives designers a powerful tool for flexible designing of structures under multi-functional requirements. Various material profiles along the thickness and in the in-plane directions are illustrated by using the 2-D power-law distribution. The effective material properties at a point are determined in terms of the local volume fractions and the material properties by the Mori-Tanaka scheme. The 2-D differential quadrature method as an efficient and accurate numerical tool is used to discretize the governing equations and to implement the boundary conditions. The fast rate of convergence of the method is shown and the results are compared against existing results in literature. Some new results for natural frequencies of the plates are prepared, which include the effects of elastic coefficients of foundation, boundary conditions, material and geometrical parameters. The interesting results indicate that a graded ceramic volume fraction in two directions has a higher capability to reduce the natural frequency than conventional 1-D functionally graded materials.

Keywords: nonlinear distribution of material profiles; 3-D vibration analysis of plates; bidirectional functionally graded materials; two-parameter elastic foundations; differential quadrature method

1. Introduction

Functionally graded materials (FGMs), a new generation of advanced composite materials, possess continuous, and smooth spatial variations of macroscopic properties such as heat conductivity, elastic modulus, mass density, etc. This is achieved by controlling the volume fraction, sizes, and shapes of material components during manufacturing. The original application of FGMs is for thermal barrier systems which are composed of heat-resisting ceramic and fracture-resisting metal with smooth transition of material properties, thus reducing cracking and delamination often observed in conventional layered systems. There have been increasingly many modern engineering applications of FGMs, such as aircraft fuselages, rocking-motor casings, packaging materials in microelectronic industry, human implants, and so.

*Corresponding author, Ph.D. Candidate, E-mail: vahid.th1982@gmail.com; v.tahouneh@iausr.ac.ir

Eraslan and Akis (2009) obtained the closed-form solution of FG rotating solid shaft and rotating solid disk under generalized plane strain and stress assumptions, respectively. Prakash and Ganapathi (2006) analyzed the asymmetric flexural vibration and thermoelastic stability of FGMs circular plates using finite element method. Efraim and Eisenberger (2007) studied the vibration of variable thickness annular isotropic plates and FG plates. Nie and Zhong (2007) investigated three-dimensional vibration of FG circular plates using semi-analytical method. Dong (2008) developed a three-dimensional free vibration analysis of FG annular plates using the Chebyshev-Ritz method. Allahverdizadeh *et al.* (2008) developed a semi-analytical approach for nonlinear free and forced axisymmetric vibrations of a thin circular FG plate, using a time averaging technique. Ebrahimi and Rastgo (2008) investigated free vibration of thin FG circular plates integrated with two piezoelectric actuator layers based on the classical plate theory. Ponnusamy and Selvamani (2012) studied the wave propagation in a generalized thermo elastic plate embedded in an elastic medium based on the Lord-Schulman (LS) and Green-Lindsay (GL) generalized two dimensional theory of thermo elasticity.

Plates on elastic foundations have been widely adopted by many researchers to study the free vibration for various engineering plate problems (Gupta *et al.* 1990, Xiang *et al.* 1994, 1996, Matsunaga 2000, Malekzadeh and Karami 2004, Zhou *et al.* 2004, 2006, Hosseini Hashemi *et al.* 2008, 2009, Ming Hung 2010, Shafiee *et al.* 2014), and limited studies have been done about the influences of elastic foundations on the free vibration of FGM plates in recent years. Malekzadeh (2009) used the differential quadrature method (DQM) for three-dimensional free vibration analysis of thick functionally graded plates on elastic foundations. Amini *et al.* (2009) described a method for the three-dimensional free vibration analysis of rectangular FGM plates resting on an elastic foundation using Chebyshev polynomials and Ritz's method. Yas and Sobhani (2010) studied free vibration characteristics of rectangular continuous grading fiber reinforced (CGFR) plates resting on elastic foundations using DQM. Recently, Tahouneh and Yas (2012) investigated the free vibration analysis of thick FG annular sector plates on Pasternak elastic foundations using DQM based on the three-dimensional elasticity theory. Hosseini-Hashemi *et al.* (2010) presented a solution to study the free vibration analysis of thin radially functionally graded annular sector plates of variable thickness on elastic foundations based on the classical plate theory (CPT) using the DQM. It can be expressed that the vibration analysis of FG circular and annular plates on elastic foundations is rare.

In the above-mentioned papers, the material properties are assumed to have a smooth variation usually in one direction. A conventional FGM may also not be so effective in such design problems since all outer surfaces of the body will have the same composition distribution. In 2003, the Columbia space shuttle was lost in a catastrophic breakup due to outer surface insulation that fell loose when the Columbia lifted off (Columbia Accident Investigation Board 2003a, b) such damage to the space shuttle's protective thermal tiles can be prevented by using FGMs. It is worth mentioning that a conventional functionally graded material may also not be so effective in such design problems since all outer surfaces of the body will have the same composition distribution and temperature distribution in such advanced machine element changes in two or three directions. Therefore, if the FGM has two-dimensional dependent material properties, a more effective high-temperature-resistant material can be obtained. Based on this fact, two-dimensional functionally graded materials (2-D FGMs) whose material properties are bidirectionally dependent are introduced.

In structural mechanics, one of the most popular semi-analytical methods is DQM (Bellman and Casti 1971), remarkable success of which has been demonstrated by many researchers in

vibration analysis of plates, shells, and beams. Liu and Liew (1999), Liew and Liu (2000) presented DQM for free vibration analysis of Mindlin isotropic circular and annular sector plates with various types of boundary conditions. A new version of the DQM was extended by Wang and Wang (2004) to analyze the free vibration of thin circular sector plates with six combinations of boundary conditions. Liew *et al.* (1996) employed DQM for free vibration analysis of moderately thick plates on Winkler foundation. Gupta *et al.* (2006) studied the free vibration analysis of non-homogeneous circular plate of non-linear thickness variation by the DQM. Nie and Zhong (2010) studied the free vibration of FG plates without elastic foundation using DQM. They assumed the material properties of the FG plate having an exponent-law variation along the thickness, radial direction or both directions. The mathematical fundamental and recent developments of differential quadrature method as well as its major applications in engineering are discussed in detail in book by Shu (2000).

This paper is motivated by the lack of studies in the technical literature concerning to the three-dimensional vibration analysis of bidirectional FG plates resting on two-parameter elastic foundations. The Mori–Tanaka scheme as an accurate micromechanics model is used for estimating the homogenized material properties. The Mori-Tanaka scheme (Mori and Tanaka 1973, Benveniste 1987, Dasgupta and Bhandarkar 1992, Hu and Weng 2000 and Genin and Birman 2009) for estimating the effective moduli is applicable to regions of the graded microstructure that have a well-defined continuous matrix and a discontinuous particulate phase. In the present paper, the differential quadrature method is employed to develop a semi-analytical solution for free vibration analyses of two-directional functionally graded annular plates resting on two-parameter elastic foundations. Simultaneous variations of the material properties in the radial and transverse directions are described by a general function. A sensitivity analysis is performed, and the natural frequencies are calculated for clamped-clamped, free-clamped and simply supported-clamped boundary conditions and different combinations of the geometric, material, and foundation parameters. Therefore, very complex combinations of the material properties, boundary conditions, and foundation stiffnesses are considered in the present semi-analytical solution approach.

2. Problem formulation

Consider a 2-D FGM annular plate which is made from a mixture of ceramics and metals as depicted in Fig. 1 The plate is supported by an elastic foundation with Winkler's (normal) and Pasternak's (shear) coefficients. The deformations defined with reference to a cylindrical coordinate system (r, θ, z) are u_r , u_θ and u_z in the r , θ and z directions, respectively. The uniform thickness, outer and inner radius of the plate are h , a and b , respectively and r_m is the mean radius of the annular plate.

2.1 Two-directional six-parameter power-law distribution

One of the well-known power-law distributions which is widely considered by the researchers is three- or four- parameter power-law distribution (Tornabene 2009, Sobhani Aragh and Yas 2010). The benefit of using such power-law distributions is to illustrate and present useful results arising from symmetric and asymmetric profiles. Consider V_c (volume fraction of the ceramic phase) is equal to $f(z)g(r)$, $f(z)$ and $g(r)$ are both the three-parameter power-law distribution. They

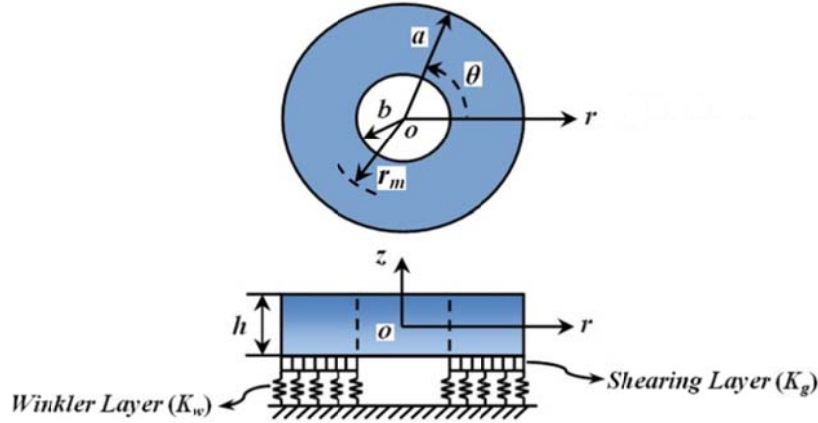


Fig. 1 A bidirectional functionally graded annular plate resting on a two-parameter elastic foundation

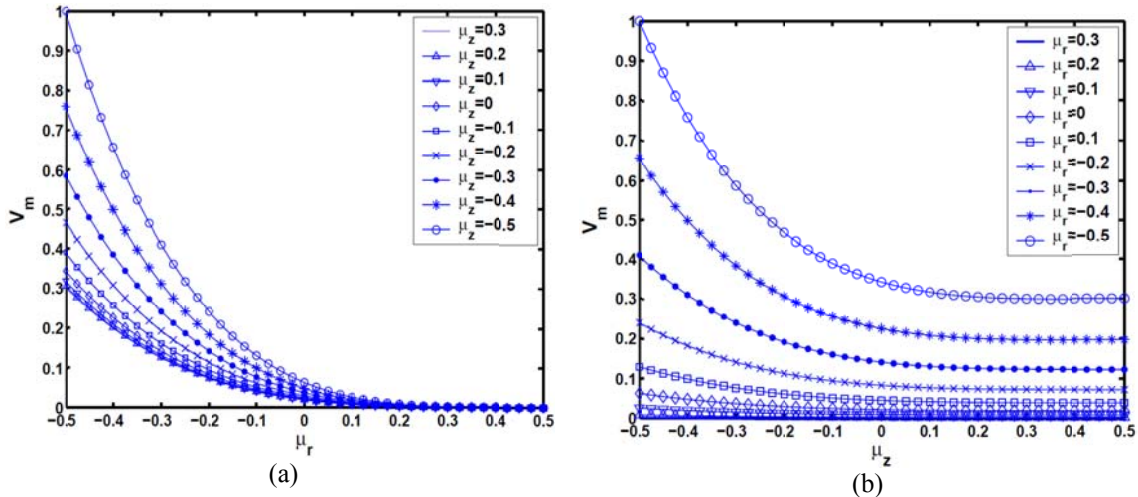


Fig. 2 Variations of the Asymmetric volume fraction profiles along the radial (μ_r) and thickness (μ_z) directions of the plate, respectively ($\gamma_r=\gamma_z=4, \alpha_r=\alpha_z=0$)

can be used to illustrate symmetric, asymmetric and classical profiles along the thickness and radial directions of the annular plate, respectively. So by considering V_c as $f(z)*g(r)$, one can present a 2-D six-parameter power-law distribution which is useful to illustrate different types of ceramic volume fraction profiles, including classical-classical, symmetric-symmetric and classical-symmetric in both directions. It should be mentioned that this equation can be used to present symmetric and asymmetric profiles in one direction (along the thickness or radial direction of the plate) as $f(z)$ or $g(r)$ is equal to one.

In this work, it is proposed that the volume fraction of the ceramic phase follows a 2-D six-parameter power-law distribution

$$V_c = (((\frac{1}{2} - \frac{z}{h}) + \alpha_z (\frac{1}{2} + \frac{z}{h})^{\beta_z})^{\gamma_z} (V_b - V_a) + V_a) (\alpha_r (\frac{1}{2} + \frac{r-r_m}{a-b})^{\beta_r} + 1 - (\frac{1}{2} + \frac{r-r_m}{a-b})^{\gamma_r}) \quad (1)$$

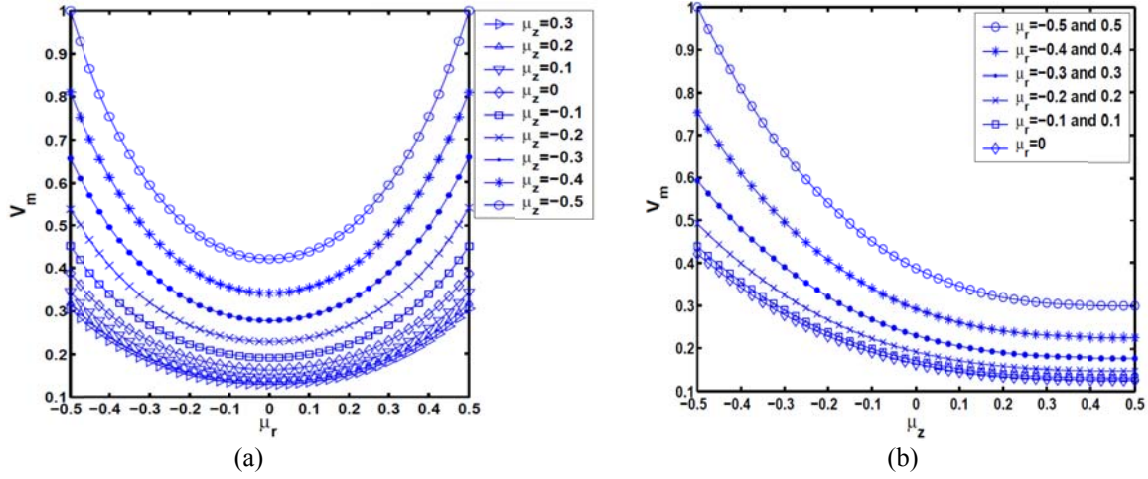


Fig. 3 Variations of the Symmetric and Asymmetric volume fraction profiles along the radial and thickness (μ_z) directions of the plate, respectively ($\gamma_r=\gamma_z=3, \alpha_r=1, \alpha_z=0, \beta_r=2$)

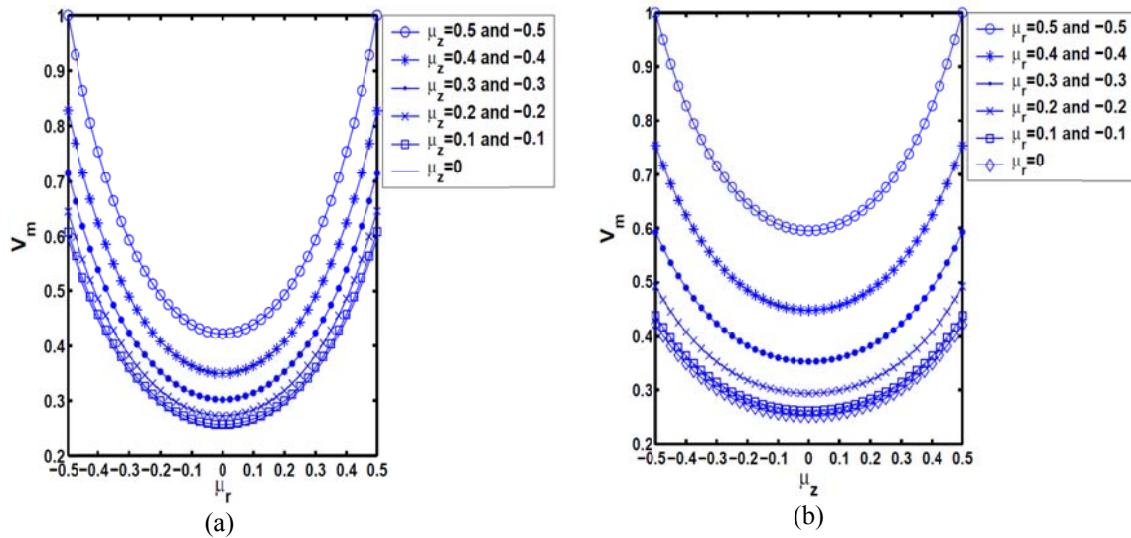


Fig. 4 Variations of the Symmetric volume fraction profiles along the radial (μ_r) and thickness (μ_z) directions of the plate, respectively ($\gamma_r=\gamma_z=3, \beta_r=\beta_z=2, \alpha_r=\alpha_z=1$)

where the radial volume fraction index γ_r , and the parameters α_r, β_r and the thickness volume fraction index γ_z , and the parameters α_z, β_z govern the material variation profile through the radial and along the thickness directions, respectively. The volume fractions V_a and V_b , which have values that range from 0 to 1, denote the ceramic volume fractions of the two different isotropic materials. For example, with assumption $V_b=1$ and $V_a=0.3$, some material profiles through the radial ($\mu_r=r-r_m/a-b$) and thickness ($\mu_z=z/h$) directions are illustrated in Figs. 2-4. As can be seen from Fig. 2, the classical volume fraction profile through the radial and thickness directions is presented as a special case of the 2-D power-law distribution (1) by setting $\gamma_r=\gamma_z=4$, and $\alpha_r=\alpha_z=0$, so in this case Eq. (1) is presented as follows

$$V_c = \left(\left(\frac{1}{2} - \mu_z\right)^4 * 0.7 + 0.3\right)\left(\frac{1}{2} - \mu_r\right)^4 \quad (2)$$

With another choice of the parameters α_r , β_r , α_z and β_z , it is possible to obtain symmetric and classical volume fraction profiles through the radial and thickness directions of the annular plate, respectively, as shown in Fig. 3. This Figure shows a classical profile versus μ_z and a symmetric profile versus μ_r . In this case Eq. (1) is presented as follows

$$V_c = \left(\left(\frac{1}{2} - \mu_z\right)^3 * 0.7 + 0.3\right)\left(\left(\frac{1}{2} + \mu_r\right)^2 + \frac{1}{2} - \mu_r\right)^3 \quad (3)$$

Fig. 4 illustrates symmetric profiles through the radial and thickness directions obtained by setting $\alpha_r = \alpha_z = 1$, $\beta_r = \beta_z = 2$ and $\gamma_r = \gamma_z = 3$

$$V_c = \left(\left(\frac{1}{2} - \mu_z + \left(\frac{1}{2} + \mu_z\right)^2\right)^3 * 0.7 + 0.3\right)\left(\left(\frac{1}{2} + \mu_r\right)^2 + \frac{1}{2} - \mu_r\right)^3 \quad (4)$$

It is also possible to obtain classical and symmetric profiles from Eq. (1) along the thickness of the plate as shown in the following equations

-Classical along the thickness of the plate ($\alpha_z = \gamma_r = 0$, $\gamma_z = 2$)

$$V_c = \left(\frac{1}{2} - \mu_z\right)^2 * 0.7 + 0.3 \quad (5)$$

-Symmetric along the thickness of the plate ($\alpha_z = 1$, $\gamma_r = 0$, $\beta_z = \gamma_z = 2$)

$$V_c = \left(\frac{1}{2} - \mu_z + \left(\frac{1}{2} + \mu_z\right)^2\right)^2 * 0.7 + 0.3 \quad (6)$$

The effective material properties of the isotropic 2-D FGMs are determined in terms of the local volume fractions and material properties of the two isotropic phases by the Mori-Tanaka scheme. It takes into account the interaction of the elastic fields among neighboring inclusions. It is assumed that the matrix phase, denoted by the subscript m , is reinforced by spherical particles of a particulate phase, denoted by the subscript c . In this notation, K_m and G_m are the bulk modulus and the shear modulus, respectively, and V_m is the volume fraction of the matrix phase. K_c , G_c , and V_c are the corresponding material properties and the volume fraction of the particulate phase. Note that $V_m + V_c = 1$, that the Lamé constant λ is related to the bulk and the shear moduli by $\lambda = K - 2G/3$, and that the stress-temperature modulus is related to the coefficient of thermal expansion by $\beta = (3\lambda + 2G)\alpha = 3K\alpha$. The following estimates for the effective local bulk modulus K and shear modulus G are useful for a random distribution of isotropic particles in an isotropic matrix

$$\frac{K - K_m}{K_c - K_m} = \frac{V_c}{1 + (1 - V_c)(K_c - K_m)/(K_m + (4/3)K_m)} \quad (7)$$

$$\frac{G - G_m}{G_c - G_m} = \frac{V_c}{1 + (1 - V_c)(G_c - G_m)/(G_m + f_m)} \quad (8)$$

where $f_m = G_m(9K_m + 8G_m)/6(K_m + 2G_m)$. The effective values of Young's modulus, E , and Poisson's ratio, ν , are found from

$$E = \frac{9KG}{3K + G}, \quad \nu = \frac{3K - 2G}{2(3K + G)} \quad (9)$$

we choose a metal/ceramic annular plate with the metal (Al) taken as the matrix phase and the ceramic (SiC) taken as the particulate phase. The material properties of aluminum and silicon carbide are listed in Table 1 (Vel and Batra 2002 and Vel 2010).

2.2 Governing equations

In the absence of body forces, the equations of motion are as follows

$$\begin{aligned} \frac{\partial \sigma_r}{\partial r} + \frac{1}{r} \frac{\partial \tau_{r\theta}}{\partial \theta} + \frac{\partial \tau_{rz}}{\partial z} + \frac{\sigma_r - \sigma_\theta}{r} &= \rho \frac{\partial^2 u_r}{\partial t^2} \\ \frac{\partial \tau_{r\theta}}{\partial r} + \frac{1}{r} \frac{\partial \sigma_\theta}{\partial \theta} + \frac{\partial \tau_{\theta z}}{\partial z} + \frac{2\tau_{r\theta}}{r} &= \rho \frac{\partial^2 u_\theta}{\partial t^2} \\ \frac{\partial \tau_{rz}}{\partial r} + \frac{1}{r} \frac{\partial \tau_{\theta z}}{\partial \theta} + \frac{\partial \sigma_z}{\partial z} + \frac{\tau_{rz}}{r} &= \rho \frac{\partial^2 u_z}{\partial t^2} \end{aligned} \quad (10)$$

σ_r , σ_θ and σ_z are normal stress components, and $\tau_{r\theta}$, $\tau_{\theta z}$ and τ_{rz} are shear stress components, u_r , u_θ and u_z are displacement components, ρ denotes material density, and t is time. The infinitesimal strain tensor is related to the displacements as follows

$$\begin{aligned} \varepsilon_r = \frac{\partial u_r}{\partial r}, \varepsilon_\theta = \frac{u_r}{r} + \frac{1}{r} \frac{\partial u_\theta}{\partial \theta}, \varepsilon_z = \frac{\partial u_z}{\partial z}, \gamma_{\theta z} = \frac{\partial u_\theta}{\partial z} + \frac{1}{r} \frac{\partial u_z}{\partial \theta}, \\ \gamma_{rz} = \frac{\partial u_r}{\partial z} + \frac{\partial u_z}{\partial r}, \gamma_{r\theta} = \frac{1}{r} \frac{\partial u_r}{\partial \theta} + \frac{\partial u_\theta}{\partial r} - \frac{u_\theta}{r} \end{aligned} \quad (11)$$

where ε_r , ε_θ , ε_z , $\gamma_{\theta z}$, $\gamma_{r\theta}$ and γ_{rz} are strain components. The mechanical constitutive relations that relate the stresses to the strains are as follows

$$\sigma_{ij} = \lambda \varepsilon_{kk} \delta_{ij} + 2\mu \varepsilon_{ij} \quad (12)$$

where λ and μ are the Lamé constants, ε_{ij} is the infinitesimal strain tensor and δ_{ij} is the Kronecker delta. Using the three-dimensional constitutive relations and the strain-displacement relations, the equations of motion in terms of displacement components with infinitesimal deformations can be written as

$$\begin{aligned} c_{11} \frac{\partial^2 u_r}{\partial r^2} + c_{12} \left(-\frac{1}{r^2} \frac{\partial u_\theta}{\partial \theta} + \frac{1}{r} \frac{\partial^2 u_\theta}{\partial r \partial \theta} + \frac{1}{r} \frac{\partial u_r}{\partial r} - \frac{1}{r^2} u_r \right) + c_{13} \frac{\partial^2 u_z}{\partial r \partial z} + \frac{\partial c_{11}}{\partial r} \frac{\partial u_r}{\partial r} + \frac{\partial c_{12}}{\partial r} \\ \left(\frac{u_r}{r} + \frac{1}{r} \frac{\partial u_\theta}{\partial \theta} \right) + \frac{\partial c_{13}}{\partial r} \frac{\partial u_z}{\partial z} + \frac{c_{66}}{r} \left[\frac{\partial^2 u_\theta}{\partial r \partial \theta} + \frac{1}{r} \frac{\partial^2 u_r}{\partial \theta^2} - \frac{1}{r} \frac{\partial u_\theta}{\partial \theta} \right] + \frac{\partial c_{55}}{\partial z} \left(\frac{\partial u_r}{\partial z} + \frac{\partial u_z}{\partial r} \right) + c_{55} \left(\frac{\partial^2 u_r}{\partial z^2} + \frac{\partial^2 u_z}{\partial z \partial r} \right) \\ + \frac{1}{r} \left[c_{11} \frac{\partial u_r}{\partial r} + c_{12} \left(\frac{u_r}{r} + \frac{1}{r} \frac{\partial u_\theta}{\partial \theta} \right) + c_{13} \frac{\partial u_z}{\partial z} - c_{12} \frac{\partial u_r}{\partial r} \right. \\ \left. - c_{22} \left(\frac{u_r}{r} + \frac{1}{r} \frac{\partial u_\theta}{\partial \theta} \right) - c_{23} \frac{\partial u_z}{\partial z} \right] = \rho \frac{\partial^2 u_r}{\partial t^2} \end{aligned} \quad (13)$$

$$\begin{aligned}
& c_{66} \left(\frac{-1}{r^2} \frac{\partial u_r}{\partial \theta} + \frac{1}{r} \frac{\partial^2 u_r}{\partial r \partial \theta} + \frac{\partial^2 u_\theta}{\partial r^2} + \frac{u_\theta}{r^2} - \frac{1}{r} \frac{\partial u_\theta}{\partial r} \right) + \frac{\partial c_{66}}{\partial r} \left(\frac{1}{r} \frac{\partial u_r}{\partial \theta} + \frac{\partial u_\theta}{\partial r} - \frac{u_\theta}{r} \right) + \\
& \frac{1}{r} (c_{12} \frac{\partial^2 u_r}{\partial \theta \partial r} + c_{22} (\frac{1}{r} \frac{\partial u_r}{\partial \theta} + \frac{1}{r} \frac{\partial^2 u_\theta}{\partial \theta^2}) + c_{23} \frac{\partial^2 u_z}{\partial \theta \partial z} + c_{44} (\frac{\partial^2 u_\theta}{\partial z^2} + \frac{1}{r} \frac{\partial^2 u_z}{\partial z \partial \theta}) + \\
& \frac{\partial c_{44}}{\partial z} (\frac{\partial u_\theta}{\partial z} + \frac{1}{r} \frac{\partial u_z}{\partial \theta}) + \frac{2c_{66}}{r} (\frac{1}{r} \frac{\partial u_r}{\partial \theta} + \frac{\partial u_\theta}{\partial r} - \frac{u_\theta}{r}) = \rho \frac{\partial^2 u_\theta}{\partial t^2}
\end{aligned} \tag{14}$$

$$\begin{aligned}
& c_{55} (\frac{\partial^2 u_r}{\partial r \partial z} + \frac{\partial^2 u_z}{\partial r^2}) + \frac{\partial c_{55}}{\partial r} (\frac{\partial u_r}{\partial z} + \frac{\partial u_z}{\partial r}) + \frac{c_{44}}{r} (\frac{\partial^2 u_\theta}{\partial \theta \partial z} + \frac{1}{r} \frac{\partial^2 u_z}{\partial \theta^2}) + c_{13} \frac{\partial^2 u_r}{\partial z \partial r} + \\
& c_{23} (\frac{1}{r} \frac{\partial u_r}{\partial z} + \frac{1}{r} \frac{\partial^2 u_\theta}{\partial \theta \partial z}) + c_{33} \frac{\partial^2 u_z}{\partial z^2} + \frac{\partial c_{13}}{\partial z} \frac{\partial u_r}{\partial r} + \frac{\partial c_{23}}{\partial z} (\frac{u_r}{r} + \frac{1}{r} \frac{\partial u_\theta}{\partial \theta}) + \frac{\partial c_{33}}{\partial z} \frac{\partial u_z}{\partial z} + \\
& \frac{c_{55}}{r} (\frac{\partial u_r}{\partial z} + \frac{\partial u_z}{\partial r}) = \rho \frac{\partial^2 u_z}{\partial t^2}
\end{aligned} \tag{15}$$

Eqs. (13)-(14) represent the in-plane equations of motion along the r and θ -axes, respectively; and Eq. (15) is the transverse or out-of-plane equation of motion. The related boundary conditions at $z=-h/2$ and $h/2$ are as follows:

at $z=-h/2$

$$\begin{aligned}
\tau_{zr} &= 0, \\
\tau_{z\theta} &= 0,
\end{aligned} \tag{16a}$$

$$\sigma_z = K_w u_z - K_g \left(\frac{\partial^2 u_z}{\partial r^2} + \frac{1}{r} \frac{\partial u_z}{\partial r} + \frac{1}{r^2} \frac{\partial^2 u_z}{\partial \theta^2} \right)$$

at $z=h/2$

$$\tau_{zr} = 0, \tau_{z\theta} = 0, \sigma_z = 0 \tag{16b}$$

K_w and K_g are Winkler and shearing layer elastic coefficients of the foundation. In this paper, three different kinds of boundary conditions are considered; Clamped-Clamped (C-C), Free-Clamped (F-C) and Simply supported-Clamped (S-C). The boundary conditions of circular edges are:

-Clamped($r=b$)-Clamped($r=a$)

$$\begin{aligned}
& \text{at } r=a \quad u_r = u_\theta = u_z = 0 \\
& \text{at } r=b \quad u_r = u_\theta = u_z = 0
\end{aligned} \tag{17}$$

-Simply supported($r=b$)-Clamped($r=a$)

$$\begin{aligned}
& \text{at } r=a \quad u_r = u_\theta = u_z = 0 \\
& \text{at } r=b \quad \sigma_r = u_\theta = u_z = 0
\end{aligned} \tag{18}$$

-Free($r=b$)-Clamped($r=a$)

$$\begin{aligned}
& \text{at } r=a \quad u_r = u_\theta = u_z = 0 \\
& \text{at } r=b \quad \sigma_r = \tau_{r\theta} = \tau_{rz} = 0
\end{aligned} \tag{19}$$

3. Solution procedure

It is necessary to develop appropriate methods to investigate the mechanical responses of 2-D FG structures. But, due to the complexity of the problem caused by the two-directional inhomogeneity, it is difficult to obtain the exact solution. In this paper, the DQM approach is used to solve the governing equations of 2-D FG annular plates. One can compare DQ solution procedure with the other two widely used traditional methods for plate analysis, i.e., Rayleigh-Ritz method and FEM. The main difference between the DQM and the other methods is how the governing equations are discretized. In DQM the governing equations and boundary conditions are directly discretized, and thus elements of stiffness and mass matrices are evaluated directly. But, in Rayleigh-Ritz and FEMs, the weak form of the governing equations should be developed and the boundary conditions are satisfied in the weak form. Generally by doing so larger number of integrals with increasing amount of differentiation should be done to arrive at the element matrices. Also, the number of degrees of freedom will be increased for an acceptable accuracy.

The basic idea of the DQM is the derivative of a function, with respect to a space variable at a given sampling point, is approximated as a weighted linear sum of the sampling points in the domain of that variable. In order to illustrate the DQ approximation, consider a function $f(\xi, \eta)$ defined on a rectangular domain $0 \leq \xi \leq a$, and $0 \leq \eta \leq b$. Let in the given domain, the function values be known or desired on a grid of sampling points. According to DQM method, the r th derivative of the function $f(\xi, \eta)$ with respect to ξ can be approximated as

$$\left. \frac{\partial^r f(\xi, \eta)}{\partial \xi^r} \right|_{(\xi, \eta) = (\xi_i, \eta_j)} = \sum_{m=1}^{N_\xi} A_{im}^{\xi(r)} f(\xi_m, \eta_j) = \sum_{m=1}^{N_\xi} A_{im}^{\xi(r)} f_{mj}$$

for $i = 1, 2, \dots, N_\xi$ and $r = 1, 2, \dots, N_\xi - 1$ (20)

From this equation one can deduce that the important components of DQM approximations are the weighting coefficients ($A_{ij}^{\xi(r)}$) and the choice of sampling points. In order to determine the weighting coefficients a set of test functions should be used in Eq. (20). The weighting coefficients for the first-order derivatives in ξ - direction are thus determined as (Bert and Malik 1996)

$$A_{ij}^{\xi} = \begin{cases} \frac{1}{a} \frac{M(\xi_i)}{(\xi_i - \xi_j)M(\xi_j)} & \text{for } i \neq j \\ -\sum_{\substack{j=1 \\ i \neq j}}^{N_\xi} A_{ij}^{\xi} & \text{for } i = j \end{cases}; i, j = 1, 2, \dots, N_\xi \quad (21)$$

Where

$$M(\xi_i) = \prod_{j=1, i \neq j}^{N_\xi} (\xi_i - \xi_j) \quad (22)$$

The weighting coefficients of the second-order derivative can be obtained as the matrix form (Bert and Malik 1996)

$$[B_{ij}^{\xi}] = [A_{ij}^{\xi}][A_{ij}^{\xi}] = [A_{ij}^{\xi}]^2 \quad (23)$$

In a similar manner, the weighting coefficients for the η -direction can be obtained.

The natural and simplest choice of the grid points is equally spaced points in the direction of the coordinate axes of computational domain. It was demonstrated that non-uniform grid points gives a better result with the same number of equally spaced grid points (Bert and Malik 1996). It is shown (Shu and Wang 1999) that one of the best options for obtaining grid points is Chebyshev–Gauss–Lobatto quadrature points

$$\frac{\xi_i}{a} = \frac{1}{2} \left\{ 1 - \cos \left[\frac{(i-1)\pi}{(N_\xi - 1)} \right] \right\}, \quad \frac{\eta_j}{b} = \frac{1}{2} \left\{ 1 - \cos \left[\frac{(j-1)\pi}{(N_\eta - 1)} \right] \right\} \quad (24a, b)$$

$$\text{for } i = 1, 2, \dots, N_\xi; j = 1, 2, \dots, N_\eta$$

Using the geometrical periodicity of the plate, the displacement components for the free vibration analysis can be represented as

$$\begin{aligned} u_r(r, \theta, z, t) &= u_{rm}(r, z) \cos(m\theta) e^{i\omega t} \\ u_\theta(r, \theta, z, t) &= u_{\theta m}(r, z) \sin(m\theta) e^{i\omega t} \\ u_z(r, \theta, z, t) &= u_{zm}(r, z) \cos(m\theta) e^{i\omega t} \end{aligned} \quad (25)$$

Where $m (=0, 1, \dots, \infty)$ is the circumferential wave number; ω is the natural frequency and $i (= \sqrt{-1})$ is the imaginary number. It is obvious that $m=0$ means axisymmetric vibration. At this stage the DQ rules are employed to discretize the free vibration equations and the related boundary conditions. Substituting for the displacement components from Eq. (25) and then using the DQ rules for the spatial derivatives, the discretized form of the equations of motion at each domain grid point (r_j, z_k) with $(j=2, 3, \dots, N_r-1)$ and $(k=2, 3, \dots, N_z-1)$ can be obtained as Eq. (13)

$$\begin{aligned} & (c_{11})_{jk} \sum_{n=1}^{N_r} B_{jn}^r u_{rmnk} + (c_{12})_{jk} \left(\frac{-u_{rmnk}}{r_j^2} + \frac{1}{r_j} \sum_{n=1}^{N_r} A_{jn}^r u_{rmnk} - \frac{m}{r_j^2} u_{\theta mnk} + \right. \\ & \left. \frac{m}{r_j} \sum_{n=1}^{N_r} A_{jn}^r u_{\theta mnk} \right) + (c_{13})_{jk} \sum_{n=1}^{N_r} \sum_{r=1}^{N_z} A_{jn}^r A_{kr}^z u_{zmnr} + \left(\frac{\partial c_{11}}{\partial r} \right)_{jk} \sum_{n=1}^{N_r} A_{jn}^r u_{rmnk} + \\ & \left(\frac{\partial c_{11}}{\partial r} \right)_{jk} \left(\frac{u_{rmjk}}{r_j} + \frac{m}{r_j} u_{\theta mj k} \right) + \left(\frac{\partial c_{13}}{\partial r} \right)_{jk} \sum_{n=1}^{N_z} A_{kn}^z u_{zmjn} + \frac{(c_{66})_{jk}}{r_j} \left(\frac{-m^2}{r_j} \right. \\ & \left. u_{rmjk} + m \sum_{n=1}^{N_r} A_{jn}^r u_{\theta mnk} - \frac{m}{r_j} u_{\theta mj k} \right) + (c_{55})_{jk} \left(\sum_{n=1}^{N_z} B_{kn}^z u_{rmjn} + \sum_{n=1}^{N_r} \sum_{r=1}^{N_z} A_{jn}^r A_{kr}^z u_{zmnr} \right) \\ & + \left(\frac{\partial c_{55}}{\partial z} \right)_{jk} \left(\sum_{n=1}^{N_z} A_{kn}^z u_{rmjn} + \sum_{n=1}^{N_r} A_{jn}^r u_{zmnk} \right) + \frac{1}{r_j} \left((c_{11})_{jk} \sum_{n=1}^{N_r} A_{jn}^r u_{rmnk} (c_{12})_{jk} \right. \\ & \left. \left(\frac{1}{r_j} u_{rmjk} + \frac{m}{r_j} u_{\theta mj k} \right) + (c_{13})_{jk} \sum_{n=1}^{N_z} A_{kn}^z u_{zmjn} - (c_{12})_{jk} \sum_{n=1}^{N_r} A_{jn}^r u_{rmnk} - (c_{22})_{jk} \right. \\ & \left. \left(\frac{1}{r_j} u_{rmjk} + \frac{m}{r_j} u_{\theta mj k} \right) - (c_{23})_{jk} \sum_{n=1}^{N_z} A_{kn}^z u_{zmjn} \right) = -\omega^2 \rho_{jk} u_{rmjk} \end{aligned} \quad (26)$$

Eq. (14)

$$\begin{aligned}
& (c_{66})_{jk} \left(\frac{m}{r_j^2} u_{rmjk} - \frac{m}{r_j} \sum_{n=1}^{N_r} A_{jn}^r u_{rmnk} + \sum_{n=1}^{N_r} B_{jn}^r u_{\theta mnk} + \frac{1}{r_j^2} u_{\theta mj k} - \frac{1}{r_j} \sum_{n=1}^{N_r} A_{jn}^r u_{\theta mnk} \right) + \\
& \left(\frac{\partial c_{66}}{\partial r} \right)_{jk} \left(-\frac{m}{r_j} u_{rmjk} + \sum_{n=1}^{N_r} A_{jn}^r u_{\theta mnk} - \frac{1}{r_j} u_{\theta mj k} \right) + \frac{1}{r_j} ((c_{12})_{jk} (-m) \sum_{n=1}^{N_r} A_{jn}^r u_{rmnk} + \\
& (c_{22})_{jk} \left(\frac{m}{r_j} u_{rmjk} - \frac{m^2}{r_j} u_{\theta mj k} \right) + (c_{23})_{jk} (-m) \sum_{n=1}^{N_z} A_{kn}^z u_{zmjn} + (c_{44})_{jk} \left(\sum_{n=1}^{N_z} B_{kn}^z u_{\theta mj n} - \right. \\
& \left. \frac{m}{r_j} \sum_{n=1}^{N_z} A_{kn}^z u_{zmjn} \right) + \left(\frac{\partial c_{44}}{\partial z} \right)_{jk} \left(\sum_{n=1}^{N_z} A_{kn}^z u_{\theta mj n} - \frac{m}{r_j} u_{zmjk} \right) + \frac{2(c_{66})_{jk}}{r_j} \left(-\frac{m}{r_j} u_{rmjk} + \right. \\
& \left. \sum_{n=1}^{N_r} A_{jn}^r u_{\theta mnk} - \frac{1}{r_j} u_{\theta mj k} \right) = -\omega^2 \rho_{jk} u_{\theta mj k}
\end{aligned} \tag{27}$$

Eq. (15)

$$\begin{aligned}
& (c_{55})_{jk} \left(\sum_{n=1}^{N_r} \sum_{r=1}^{N_z} A_{kr}^z A_{jn}^r u_{rmnr} + \sum_{n=1}^{N_r} B_{jn}^r u_{zmnk} \right) + \left(\frac{\partial c_{55}}{\partial r} \right)_{jk} \left(\sum_{n=1}^{N_z} A_{kn}^z u_{rmjn} + \right. \\
& \left. \sum_{r=1}^{N_r} A_{jr}^r u_{zmrk} \right) + \frac{(c_{44})_{jk}}{r_j} \left(m \sum_{n=1}^{N_z} A_{kn}^z u_{\theta mj n} - \frac{m^2}{r_j} u_{zmjk} \right) + (c_{13})_{jk} \\
& \left(\sum_{n=1}^{N_r} \sum_{r=1}^{N_z} A_{kr}^z A_{jn}^r u_{rmnr} \right) + (c_{23})_{jk} \left(\frac{m}{r_j} \sum_{n=1}^{N_z} A_{kn}^z u_{\theta mj n} + \frac{1}{r_j} \sum_{n=1}^{N_z} A_{kn}^z u_{rmjn} \right) + \\
& (c_{33})_{jk} \sum_{n=1}^{N_z} B_{kn}^z u_{zmjn} + \left(\frac{\partial c_{13}}{\partial z} \right)_{jk} \sum_{n=1}^{N_r} A_{jn}^r u_{rmnk} + \left(\frac{\partial c_{23}}{\partial z} \right)_{jk} \left(\frac{u_{rmjk}}{r_j} + \frac{m}{r_j} u_{\theta mj k} \right) + \\
& \left(\frac{\partial c_{33}}{\partial z} \right)_{jk} \sum_{n=1}^{N_z} A_{kn}^z u_{zmjn} + \frac{(c_{55})_{jk}}{r_j} \left(\sum_{n=1}^{N_z} A_{kn}^z u_{rmjn} + \sum_{r=1}^{N_r} A_{jr}^r u_{zmrk} \right) = -\omega^2 \rho_{jk} u_{zmjk}
\end{aligned} \tag{28}$$

where A_{ij}^r , A_{ij}^z and B_{ij}^r , B_{ij}^z are the first and second order differential quadrature weighting coefficients in the r - and z - directions, respectively. u_{rmjk} , $u_{\theta mj k}$ and u_{zmjk} represent the displacement components of the node (j, k) defined by $r=r_j$ and $z=z_k$. Also, N_r and N_z represent the total number of nodes through the radial and thickness of the plate, respectively. In a similar manner the boundary conditions can be discretized. For this purpose, using Eq. (20) and the differential quadrature discretization rules for spatial derivatives, the boundary conditions at $z = -h/2$ and $h/2$ become,

Eq. (16a)

$$\begin{aligned}
& \sum_{n=1}^{N_z} A_{kn}^z u_{rmjn} + \sum_{n=1}^{N_r} A_{jn}^r u_{zmnk} = 0, \quad \frac{-m}{r_j} u_{zmjk} + \sum_{n=1}^{N_z} A_{kn}^z u_{\theta mj n} = 0, \\
& (c_{13})_{jk} \sum_{n=1}^{N_r} A_{jn}^r u_{rmnk} + (c_{23})_{jk} \left(\frac{u_{rmjk}}{r_j} + \frac{m}{r_j} u_{\theta mj k} \right) + (c_{33})_{jk} \sum_{n=1}^{N_z} A_{kn}^z u_{zmjn} \\
& -K_{\omega} u_{zmjk} + K_g \left(\sum_{n=1}^{N_r} B_{jn}^r u_{zmnk} + \frac{1}{r_j} \sum_{n=1}^{N_r} A_{jn}^r u_{zmnk} - \frac{m^2}{r_j^2} u_{zmjk} \right) = 0
\end{aligned} \tag{29a}$$

Eq. (16b)

$$\sum_{n=1}^{N_z} A_{kn}^z u_{rmjn} + \sum_{n=1}^{N_r} A_{jn}^r u_{zmnk} = 0, \frac{-m}{r_j} u_{zmjk} + \sum_{n=1}^{N_z} A_{kn}^z u_{\theta mjn} = 0, \quad (29b)$$

$$(c_{13})_{jk} \sum_{n=1}^{N_r} A_{jn}^r u_{rmnk} + (c_{23})_{jk} \left(\frac{u_{rmjk}}{r_j} + \frac{m}{r_j} u_{\theta mjk} \right) + (c_{33})_{jk} \sum_{n=1}^{N_z} A_{kn}^z u_{zmjn} = 0$$

where $k=1$ at $z=-h/2$ and $k=N_z$ at $z=h/2$, and $j=1, 2, \dots, N_r$.

The boundary conditions at $r=b$ and a stated in Eqs. (17)-(19) become,

-Simply supported (S)

$$u_{\theta mjk} = 0, u_{zmjk} = 0, \quad (30a)$$

$$(c_{11})_{jk} \sum_{n=1}^{N_r} A_{jn}^r u_{rmnk} + (c_{12})_{jk} \left(\frac{u_{rmjk}}{r_j} + \frac{m}{r_j} u_{\theta mjk} \right) + (c_{13})_{jk} \sum_{n=1}^{N_z} A_{kn}^z u_{zmjn} = 0$$

-Clamped (C)

$$u_{rmjk} = 0, u_{\theta mjk} = 0, u_{zmjk} = 0 \quad (30b)$$

-Free (F)

$$(c_{11})_{jk} \sum_{n=1}^{N_r} A_{jn}^r u_{rmnk} + (c_{12})_{jk} \left(\frac{u_{rmjk}}{r_j} + \frac{m}{r_j} u_{\theta mjk} \right) + (c_{13})_{jk} \sum_{n=1}^{N_z} A_{kn}^z u_{zmjn} = 0, \quad (30c)$$

$$\sum_{n=1}^{N_r} A_{jn}^r u_{\theta mnk} - \frac{m}{r_j} u_{rmjk} - \frac{1}{r_j} u_{\theta mjk} = 0,$$

$$\sum_{n=1}^{N_z} A_{kn}^z u_{rmjn} + \sum_{n=1}^{N_r} A_{jn}^r u_{zmnk} = 0$$

In the above equations $k=2, \dots, N_z-1$; also $j=1$ at $r=b$ and $j=N_r$ at $r=a$.

In order to carry out the eigenvalue analysis, the domain and boundary nodal displacements should be separated. In vector forms, they are denoted as $\{d\}$ and $\{b\}$, respectively. Based on this definition, the discretized form of the equations of motion and the related boundary conditions can be represented in the matrix form as:

Equations of motion Eqs. (26)-(28)

$$\left[\begin{matrix} [K_{db}] & [K_{dd}] \end{matrix} \right] \begin{Bmatrix} \{b\} \\ \{d\} \end{Bmatrix} - \omega^2 [M] \{d\} = \{0\} \quad (31)$$

Boundary conditions Eqs. (29a)-(29b) and Eqs. (30a)-(30c)

$$[K_{bd}] \{d\} + [K_{bb}] \{b\} = \{0\} \quad (32)$$

Eliminating the boundary degrees of freedom in Eq. (31) using Eq. (32), this equation becomes

$$[K] - \omega^2 [M] \{d\} = \{0\} \quad (33)$$

where $[K]=[K_{dd}]-[K_{db}][K_{bb}]^{-1}[K_{bd}]$. The above eigenvalue system of equations can be solved to find the natural frequencies and mode shapes of the plate.

4. Numerical results and discussion

Due to lack of appropriate results for free vibration of 2-D FG annular plates for direct comparison, validation of the presented formulation is conducted in two ways. Firstly, the results are compared with those of 1-D conventional functionally graded annular plates, and then, the results of the presented formulations are given in the form of convergence studies with respect to N_z and N_r , the number of discrete points distributed along the thickness and radial directions, respectively.

As a first example, it is assumed that the material properties have the following exponential distributions in the thickness direction of the plate

$$c_{ij}(z) = c_{ij}^C e^{\left(\frac{\lambda z}{h}\right)}, \rho(z) = \rho^C e^{\left(\frac{\lambda z}{h}\right)} \quad (34)$$

-Ceramic (Alumina, Al_2O_3)

$$E^C = 380 * 10^9 \text{ N/m}^2, \rho^C = 3,800 \text{ kg/m}^3, \nu = 0.3.$$

where the superscript C refers to the material properties of the bottom surface and λ is the material property graded index.

In Table 2, the first non-dimensional natural frequency parameters for the simply supported-clamped functionally graded annular plates are compared with those of Nie and Zhong (2007) and Dong (2008). As the second example, the first three non-dimensional frequencies for FG annular plates with clamped inner and outer edges for different circumferential wave number (m) are compared with those of the three-dimensional elasticity solution of Nie and Zhong (2010) in Table 3.

As another example, based on the power law distribution, the Young's modulus E and the mass density ρ are assumed to be in terms of a power law distribution as follows

$$E(z) = E_C + E_{CM} V_f, \rho(z) = \rho_C + \rho_{CM} V_f \quad (35)$$

$$E_{CM} = E_M - E_C, \rho_{CM} = \rho_M - \rho_C, V_f = (z/h)^g \quad (36)$$

where h is the thickness of the plate and g is the power law index which takes values greater than or equal to zero. Subscripts M and C refer to the metal and ceramic constituents which denote the material property of the top and bottom surface of the plate, respectively. The material properties are as follows:

-Metal (Aluminum, Al):

$$E_M = 70 * 10^9 \text{ N/m}^2, \nu = 0.3, \rho_M = 2702 \text{ kg/m}^3$$

Table 1 Material properties of aluminum and silicon carbide

| | Young's Modulus, E (Gpa) | Poisson's ratio, ν | Mass density, ρ (kg/m ³) |
|-----------------------|----------------------------|------------------------|---|
| Al | 70 | 0.30 | 2,707 |
| Silicon carbide (Sic) | 410 | 0.170 | 3,100 |

Table 2 Convergence results of the first non-dimensional natural frequency parameters ($\varpi = \omega h \sqrt{\rho/C_{11}}, C_{11} = E(1-\nu)/(1+\nu)(1-2\nu)$) for functionally graded annular plates with simply supported ($r=b$) and clamped ($r=a$) edges ($a=1$ m, $b=0.1$, $h/a=0.2$)

| $N_r=N_z$ | wave number (m) | λ | | | | |
|-------------------------------------|----------------------|----------------------|--------|--------|--------|--------|
| | | 1 | 5 | 10 | 15 | |
| (Dong 2008) (Nie and Zhong 2007) | 0 | 7 | 0.1886 | 0.1331 | 0.0784 | 0.0529 |
| | | 9 | 0.1873 | 0.1318 | 0.0783 | 0.0536 |
| | | 11 | 0.1872 | 0.1316 | 0.0782 | 0.0534 |
| | | 13 | 0.1872 | 0.1314 | 0.0782 | 0.0535 |
| | | 17 | 0.1870 | 0.1315 | 0.0781 | 0.0534 |
| | | (Dong 2008) | 0.1871 | 0.1315 | 0.0780 | 0.0536 |
| | | (Nie and Zhong 2007) | 0.1936 | - | - | - |
| | 1 | 7 | 0.1801 | 0.1313 | 0.0733 | 0.0475 |
| | | 9 | 0.1972 | 0.1394 | 0.0809 | 0.0576 |
| | | 11 | 0.1990 | 0.1401 | 0.0821 | 0.0579 |
| | | 13 | 0.1990 | 0.1401 | 0.0852 | 0.0581 |
| | | 17 | 0.1993 | 0.1402 | 0.0842 | 0.0582 |
| | | (Dong 2008) | 0.1994 | 0.1402 | 0.0840 | 0.0582 |
| | | (Nie and Zhong 2007) | 0.2050 | - | - | - |
| | 2 | 7 | 0.2744 | 0.1955 | 0.1227 | 0.0851 |
| | | 9 | 0.2748 | 0.1968 | 0.1202 | 0.0842 |
| | | 11 | 0.2785 | 0.1973 | 0.1201 | 0.0832 |
| 13 | | 0.2783 | 0.1969 | 0.1201 | 0.0831 | |
| 17 | | 0.2782 | 0.1967 | 0.1187 | 0.0823 | |
| (Dong 2008) | | 0.2781 | 0.1967 | 0.1184 | 0.0820 | |
| (Nie and Zhong 2007) | | 0.2684 | - | - | - | |
| 3 | 7 | 0.3831 | 0.277 | 0.1715 | 0.1188 | |
| | 9 | 0.3824 | 0.2765 | 0.1697 | 0.1184 | |
| | 11 | 0.3824 | 0.2757 | 0.1696 | 0.1180 | |
| | 13 | 0.3819 | 0.2757 | 0.1692 | 0.1181 | |
| | 17 | 0.3819 | 0.2752 | 0.1692 | 0.1182 | |
| | (Dong 2008) | 0.3819 | 0.2751 | 0.1693 | 0.1182 | |
| | (Nie and Zhong 2007) | - | - | - | - | |

Table 3 Convergence results of the first three non-dimensional frequencies for functionally graded annular plates with Clamped-Clamped edges ($a=1$ m, $b=0.2$, $\lambda=1$)

| wave number (m) | Number of the discrete point along the radial and thickness directions while using DQM | | | | | | |
|--------------------|--|--------|--------|--------|--------|----------------------|--------|
| | 7 | 9 | 11 | 13 | 17 | (Nie and Zhong 2010) | Ansys* |
| 0 | 0.094 | 0.0856 | 0.0816 | 0.0801 | 0.0806 | 0.0807 | 0.0810 |
| 1 | 0.1006 | 0.0896 | 0.0844 | 0.0831 | 0.0838 | 0.0837 | 0.0839 |
| 2 | 0.1147 | 0.1027 | 0.0977 | 0.0955 | 0.0961 | 0.0961 | 0.0963 |

* Nie and Zhong (2010)

-Ceramic (Alumina, Al_2O_3):

$$E_C = 380 * 10^9 \text{ N/m}^2, \nu = 0.3, \rho_C = 3800 \text{ kg/m}^3.$$

In Tables 4 and 5, the results for FG annular plates are compared with those of Dong (2008) for different values of the power law index and circumferential wave number (m).

Table 4 Convergence study of the first five non-dimensional natural frequency parameters ($\varpi = \omega a \sqrt{\rho/G_m}$) for free vibration of a Clamped-Clamped functionally graded annular plate ($a/b=2.5$ m, $h/a=0.5$, $g=1$)

| $N_r=N_z$ | wave number (m) | ϖ_1 | ϖ_2 | ϖ_3 | ϖ_4 | ϖ_5 |
|-------------|---------------------|------------|------------|------------|------------|------------|
| 7 | 0 | 8.177 | 13.912 | 15.516 | 19.446 | 20.108 |
| 9 | | 8.201 | 13.875 | 15.511 | 19.481 | 20.158 |
| 11 | | 8.208 | 13.867 | 15.511 | 19.484 | 20.162 |
| 13 | | 8.210 | 13.870 | 15.511 | 19.485 | 20.164 |
| 17 | | 8.213 | 13.872 | 15.515 | 19.485 | 20.166 |
| (Dong 2008) | | 8.214 | 13.872 | 15.514 | 19.485 | 20.167 |
| 7 | 1 | 8.303 | 9.696 | 13.803 | 14.885 | 15.546 |
| 9 | | 8.322 | 9.689 | 13.769 | 14.853 | 15.533 |
| 11 | | 8.327 | 9.688 | 13.767 | 14.851 | 15.533 |
| 13 | | 8.329 | 9.688 | 13.765 | 14.850 | 15.533 |
| 17 | | 8.332 | 9.689 | 13.766 | 14.849 | 15.536 |
| (Dong 2008) | | 8.333 | 9.689 | 13.766 | 14.850 | 15.535 |
| 7 | 2 | 8.849 | 11.160 | 13.842 | 15.638 | 16.561 |
| 9 | | 8.861 | 11.147 | 13.814 | 15.615 | 16.548 |
| 11 | | 8.863 | 11.146 | 13.812 | 15.615 | 16.549 |
| 13 | | 8.865 | 11.145 | 13.810 | 15.614 | 16.549 |
| 17 | | 8.868 | 11.145 | 13.811 | 15.614 | 16.550 |
| (Dong 2008) | | 8.869 | 11.145 | 13.810 | 15.615 | 16.550 |
| 7 | 3 | 9.901 | 12.693 | 14.423 | 16.390 | 17.699 |
| 9 | | 9.906 | 12.681 | 14.399 | 16.422 | 17.714 |
| 11 | | 9.919 | 12.670 | 14.402 | 16.451 | 17.718 |
| 13 | | 9.921 | 12.673 | 14.407 | 16.453 | 17.720 |
| 17 | | 9.923 | 12.673 | 14.407 | 16.456 | 17.721 |
| (Dong 2008) | | 9.924 | 12.672 | 14.407 | 16.455 | 17.721 |

Table 5 Convergence study of the first five non-dimensional natural frequency parameters ($\varpi = \omega a \sqrt{\rho/G_m}$) for free vibration of a clamped-clamped functionally graded annular plate ($a/b=2.5$, $h/a=0.5$, $g=5$)

| $N_r=N_z$ | wave number (m) | ϖ_1 | ϖ_2 | ϖ_3 | ϖ_4 | ϖ_5 |
|-------------|---------------------|------------|------------|------------|------------|------------|
| 7 | 0 | 10.063 | 18.379 | 19.726 | 24.456 | 25.726 |
| 9 | | 10.087 | 18.342 | 19.720 | 24.421 | 25.786 |
| 11 | | 10.094 | 18.333 | 19.721 | 24.424 | 25.790 |
| 13 | | 10.096 | 18.336 | 19.721 | 24.425 | 25.792 |
| 17 | | 10.098 | 18.338 | 19.723 | 24.427 | 25.794 |
| (Dong 2008) | | 10.099 | 18.338 | 19.724 | 24.426 | 25.794 |
| 7 | 1 | 10.237 | 12.343 | 18.229 | 18.615 | 19.676 |
| 9 | | 10.256 | 12.336 | 18.195 | 18.583 | 19.653 |
| 11 | | 10.261 | 12.335 | 18.193 | 18.580 | 19.649 |
| 13 | | 10.263 | 12.335 | 18.191 | 18.578 | 19.649 |
| 17 | | 10.267 | 12.336 | 18.191 | 18.579 | 19.651 |
| (Dong 2008) | | 10.266 | 12.336 | 18.192 | 18.578 | 19.651 |
| 7 | 2 | 10.917 | 14.407 | 18.479 | 18.514 | 20.715 |

Table 5 Continued

| | | | | | | |
|-------------|---|--------|--------|--------|--------|--------|
| 9 | | 10.929 | 14.394 | 18.451 | 18.490 | 20.702 |
| 11 | | 10.931 | 14.393 | 18.449 | 19.490 | 20.703 |
| 13 | | 10.933 | 14.392 | 18.447 | 19.489 | 20.703 |
| 17 | | 10.936 | 14.392 | 18.448 | 19.489 | 20.704 |
| (Dong 2008) | | 10.937 | 14.392 | 18.448 | 19.490 | 20.704 |
| 7 | 3 | 12.178 | 16.685 | 19.325 | 20.630 | 22.402 |
| 9 | | 12.228 | 16.673 | 19.301 | 20.662 | 22.413 |
| 11 | | 12.241 | 16.662 | 19.304 | 20.691 | 22.418 |
| 13 | | 12.243 | 16.665 | 19.309 | 20.693 | 22.420 |
| 17 | | 12.247 | 16.664 | 19.310 | 20.694 | 22.421 |
| (Dong 2008) | | 12.246 | 16.664 | 19.310 | 20.695 | 22.421 |

Table 6 Various ceramic volume fraction profiles, different parameters, and volume fraction indices of two-dimensional power-law distributions.

| Volume fraction profile | The thickness volume fraction index and parameters | The radial volume fraction index and parameters |
|---------------------------------|--|---|
| Classical-Classical | $\alpha_z=0$ | $\alpha_r=0$ |
| Symmetric-Symmetric | $\alpha_z=1, \beta_z=2$ | $\alpha_r=1, \beta_r=2$ |
| Classical- Symmetric | $\alpha_z=0$ | $\alpha_z=1, \beta_z=2$ |
| Classical through the thickness | $\alpha_z=0$ | $\gamma_r=0$ |
| Symmetric through the thickness | $\alpha_z=1, \beta_z=2$ | $\gamma_r=0$ |

According to the data presented in the above-mentioned tables, excellent solution agreements can be observed between the present method and those of the other methods. Based on the above studies, a numerical value of $N_r=N_z=17$ is used for the next studies.

After demonstrating the convergence and accuracy of the method, parametric studies for 3-D vibration analysis of bidirectional FG annular plates for different types of ceramic volume fraction profiles and various thickness to outer radius ratio (h/a) and different combinations of free, simply supported and clamped boundary conditions at the circular edges, are computed. The non-dimensional natural frequency, Winkler and shearing layer elastic coefficients are as follows

$$\Omega = \omega a^2 \sqrt{\rho_{Al} h / D_{Al}}, D_{Al} = E_{Al} h^3 / 12(1 - \nu_{Al}^2) \tag{37}$$

$$k_g = K_g a^2 / D_{Al}, k_w = K_w a^4 / D_{Al} \tag{38}$$

where ρ_{Al} , E_{Al} and ν_{Al} are mechanical properties of aluminum. It should be noted that the two-dimensional functionally graded annular plates considered in this work are assumed to be composed of aluminum and silicon carbide. In the following, we have compared the several different ceramic volume fraction profiles of conventional 1-D and 2-D FGMs with appropriate choice of the radial and thickness parameters of the 2-D six-parameter power-law distribution, as shown in Table 6. It should be noted that the notation Classical- Symmetric indicates that the 2-D FG annular plate has classical and symmetric volume fraction profiles through the thickness and radial directions, respectively.

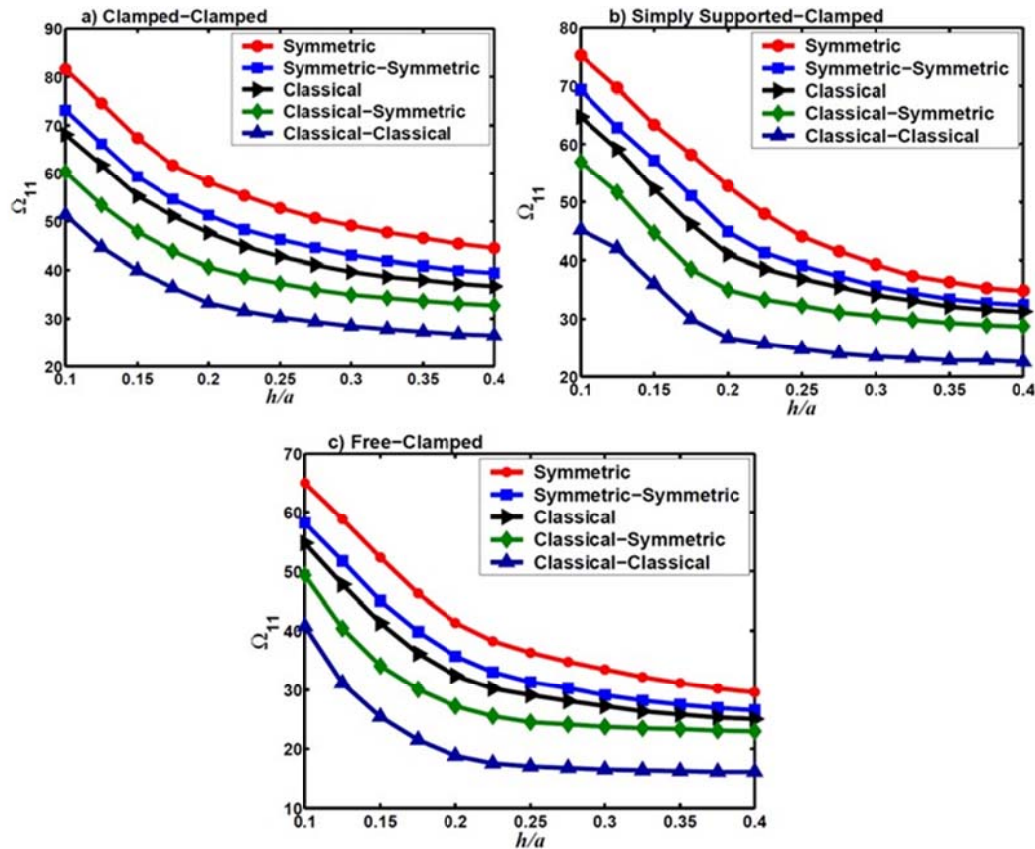


Fig. 5 Variations of fundamental frequency parameters of two-dimensional functionally graded annular plates resting on an elastic foundation with h/a ratio for different volume fraction profiles and various boundary conditions ($K_r=K_w=100$, $\gamma_z=2$, $b/a=0.2$)

The variations of fundamental frequency parameters of 2-D FG annular plates resting on an elastic foundation with thickness to outer radius ratio (h/a) for different types of volume fraction profiles and boundary conditions are depicted in Fig. 5. It can also be inferred from Fig. 5 that the frequency is greatly influenced in that fundamental frequency parameter decreases steadily as (h/a) ratio becomes larger. As can be seen from Fig. 5, for the all thickness to outer radius ratio (h/a), Classical-Classical volume fractions profile has the lowest frequencies followed by Classical-Symmetric, Classical, Symmetric-Symmetric and Symmetric profiles.

The effect of different types of ceramic volume fraction profiles on the frequency parameters of S-C bidirectional annular plates for different values of circumferential wave number (m) is shown in Fig. 6. According to this figure, the lowest frequency parameter is obtained by using Classical-Classical volume fractions profile. On the contrary, the 1-D FG annular plate with symmetric volume fraction profiles has the maximum value of the frequency parameter. Therefore, a graded ceramic volume fraction in two directions has high capabilities to reduce the frequency parameter than conventional 1-D FGM. Moreover, in Fig. 6, the interesting results show that, with increasing values of the circumferential wave number (m), frequency parameter of the Classical FGM annular plate is close to that of a Symmetric-Symmetric. Therefore, it can be concluded that using 2-D six-

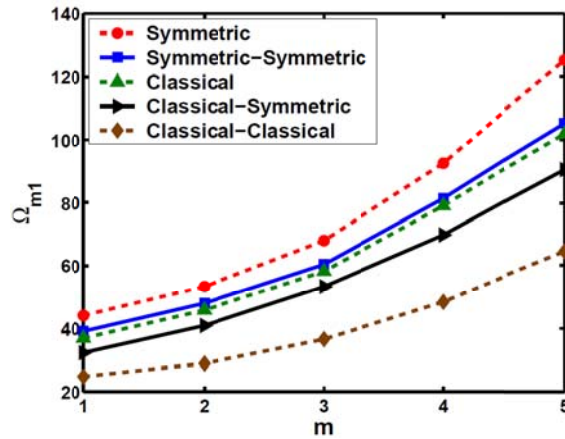


Fig. 6 Variation of the frequency parameters versus circumferential wave numbers (m) with different volume fraction profiles for S-C annular plates resting on an elastic foundation ($K_r=K_w=100, \gamma_z=2, h/a=0.25, b/a=0.2$)

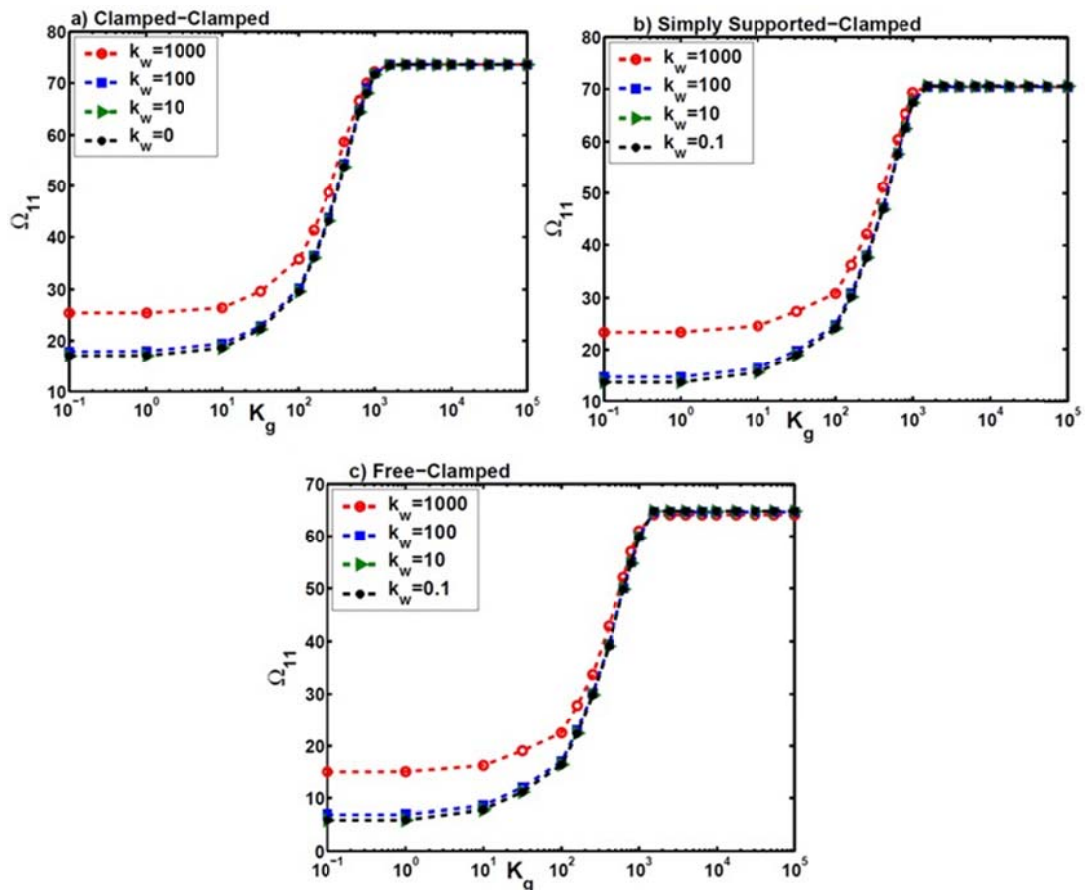


Fig. 7 Variation of the fundamental frequency parameters of two-dimensional functionally graded annular plates resting on an elastic foundation versus the shearing layer elastic coefficient for different Winkler elastic coefficient and different boundary conditions ($\alpha_r=\alpha_z=0, \gamma_z=\gamma_r=2, h/a=0.25, b/a=0.2$)

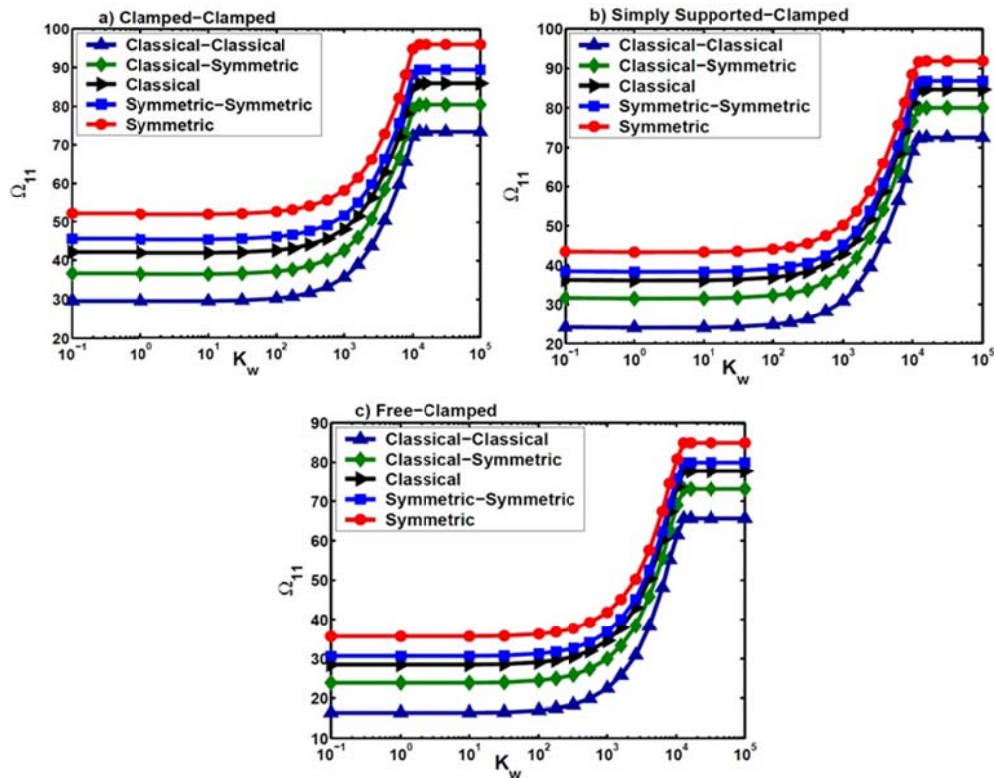


Fig. 8 Variations of fundamental frequency parameters of two-dimensional functionally graded annular plates resting on an elastic foundation with Winkler elastic coefficient for different volume fraction profiles and various boundary conditions ($K_g=100$, $h/a=0.25$, $\gamma_z=2$, $b/a=0.2$)

parameter power-law distribution leads to a more flexible design so that maximum or minimum value of natural frequency can be obtained to a required manner.

The influence of shearing layer elastic coefficient on the fundamental frequency parameters for three sets of boundary conditions is shown in Fig. 7. It results the variation of Winkler elastic coefficient has little effect on the non-dimensional natural frequencies at different values of shearing layer elastic coefficient. It is clear that in all cases, with increasing the elastic coefficients of the foundation, the frequency parameters increase to some limit values. It is observed for the large values of shearing layer elastic coefficient, the results become independent of it. The effect of the Winkler elastic coefficient on the fundamental frequency parameters at different values of the shearing layer elastic coefficient with different boundary conditions is shown in Fig. 8. It is observed that the fundamental frequency parameters converge with increasing Winkler elastic coefficient of the foundation. According to this figure, the lowest frequency parameter is obtained by using Classical-Classical volume fractions profile. On the contrary, the 1-D FG annular plate with symmetric volume fraction profiles has the maximum value of the frequency parameter. The variations of fundamental frequency parameters of 2-D FG annular plates with thickness-to-outer radius ratio (h/a), and the volume fraction index through the thickness of the plates for F-C boundary condition are shown in Fig. 9, by considering ($\alpha_z=\alpha_r=0$, $\gamma_r=2$, $k_g=k_w=100$) for Classical-Classical 2-D FG plates. As it is observed, the fundamental frequency parameter decreases rapidly

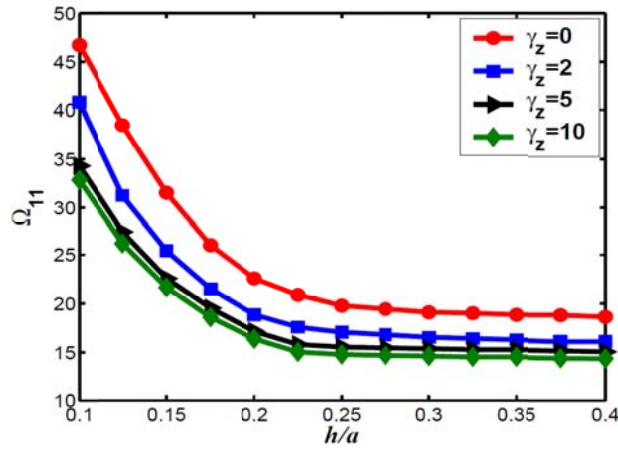


Fig. 9 Variations of fundamental frequency parameters of F-C two-dimensional functionally graded annular plates with h/a ratio and the volume fraction index through thickness of the plate ($K_w=K_g=100, \alpha_r=\alpha_z=0, \gamma_r=2, b/a=0.2$)

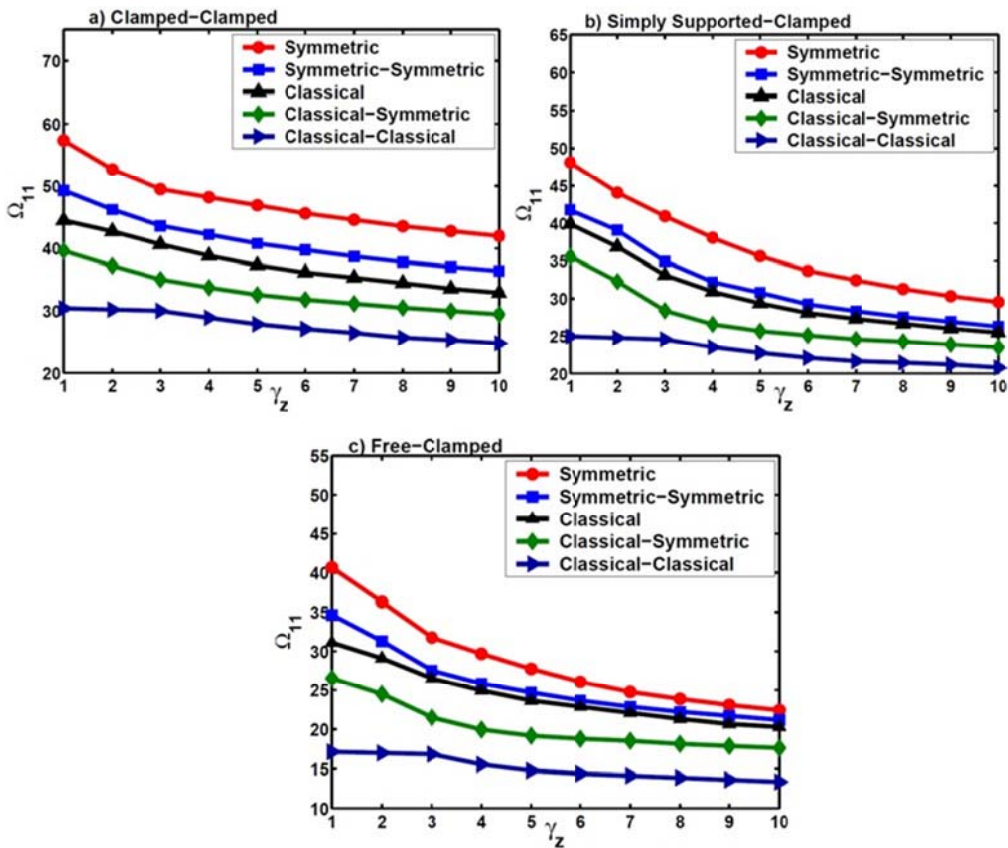


Fig. 10 Effect of the volume fraction index through the thickness direction (γ_z) on the fundamental frequency parameters of two-dimensional functionally graded annular plates resting on an elastic foundation for different volume fraction profiles and various boundary conditions ($K_g=K_w=100, h/a=0.25, b/a=0.2$)

with the increase of the h/a ratio and then remains almost unaltered for the large values of thickness-to outer radius ratio ($h/a > 0.25$). This behavior is also observed for other boundary conditions, not shown here for brevity. It is found that for the all boundary conditions the frequency parameter decreases by increasing the thickness volume fraction index, due to the fact that the silicon carbide fraction decreases, and as we know silicon carbide has a much higher Young's modulus than aluminum.

Now we study the influence of various types of the ceramic volume fraction profile on the fundamental natural frequency at various volume fraction indices through the thickness direction (γ_z) of the annular plates (Fig. 10). The results show that the fundamental natural frequency decreases rapidly and then approaches a constant value for higher values of the volume fraction index through the thickness of the plates. It is also seen that the thickness volume fraction index has less effect on the frequency parameter for the Classical-Classical volume fraction profile.

5. Conclusions

In this research work, differential quadrature method is employed to obtain a highly accurate semi-analytical solution for the three-dimensional free vibration of bidirectional annular plates resting on a two-parameter elastic foundation under various boundary conditions. The study is carried out based on the three-dimensional, linear and small strain elasticity theory. Various material profiles through radial and thickness directions are illustrated using the 2-D power-law distribution. The effective material properties at a point are determined in terms of the local volume fractions and material properties by the Mori-Tanaka scheme. The effects of different boundary conditions, various geometrical parameters, different ceramic volume fraction profiles in the thickness and radial directions and elastic coefficients of foundation of bidirectional annular plates resting on a two-parameter elastic foundation are investigated. Moreover, vibration behavior of 2-D FG plates is compared with one-dimensional conventional 1-D FG plates. From this study, some conclusions can be made:

- It results the variation of Winkler elastic coefficient has little effect on the non-dimensional natural frequencies at different values of shearing layer elastic coefficient. One can see that in all cases (Fig. 7), with increasing the shearing layer elastic coefficient of the foundation, the frequency parameters increase to some limit values. It is observed for the large values of shearing layer elastic coefficient, the results become independent of it.

- The non-dimensional natural frequency parameters converge with increasing Winkler elastic coefficient of the foundation, it should be noted that non-dimensional natural frequency parameters converge at the large values of the Winkler elastic coefficient.

- The results show that the fundamental natural frequency decreases rapidly and then approaches a constant value for higher values of the thickness volume fraction index. It is also seen that the thickness volume fraction index exerts an insignificant influence on the frequency parameter for the Classical-Classical volume fraction profile.

- It is found that for the all boundary conditions the frequency parameter decreases by increasing the thickness volume fraction index, due to the fact that the silicon carbide fraction decreases, and as we know silicon carbide has a much higher Young's modulus than aluminum.

- The interesting results show that the lowest magnitude frequency parameter is obtained by using a Classical-Classical volume fractions profile. It can be concluded that a graded ceramic volume fraction in two directions has higher capabilities to reduce the natural frequency than a

conventional 1-D FGM. Moreover, the results show that with increasing values of the circumferential wave number (m), frequency parameter of the Classical FGM annular plate is close to that of a Symmetric-Symmetric.

Based on the achieved results, using 2-D six-parameter power-law distribution leads to a more flexible design so that maximum or minimum value of natural frequency can be obtained to a required manner.

References

- Allahverdizadeh, A., Naei, M.H. and Nikkhah Bahrami M. (2008), "Nonlinear free and forced vibration analysis of thin circular functionally graded plates", *J. Sound Vib.*, **310**(4-5), 966-984.
- Amini, M.H., Soleimani, M. and Rastgoo, A. (2009), "Three-dimensional free vibration analysis of functionally graded material plates resting on an elastic foundation", *Smart Mater. Struct.*, **18**(8), 085015.
- Bellman, R. and Casti, J. (1971), "Differential quadrature and long term integration", *J. Math. Anal. Appl.*, **34**(2), 235-238.
- Benveniste, Y. (1987), "A new approach to the application of Mori-Tanaka's theory of composite materials", *Mech. Mater.*, **6**(2), 147-157.
- Bert, C.W. and Malik, M. (1996), "Differential quadrature method in computational mechanics, a review", *Appl. Mech. Rev.*, **49**(1), 1-27.
- Columbia Accident Investigation Board (2003a), *Report of Columbia Accident Investigation Board*, Vol. I. NASA.
- Columbia Accident Investigation Board (2003b), *In-Flight Options Assessment*, Vol. II. NASA, Appendix D.12 (PDF).
- Dasgupta, A. and Bhandarkar, S.M. (1992), "A generalized self-consistent Mori-Tanaka scheme for fiber-composites with multiple inter-phases", *Mech. Mater.*, **14**(1), 67-82.
- Dong, C.Y. (2008), "Three-dimensional free vibration analysis of functionally graded annular plates using the Chebyshev-Ritz method", *Mater. Des.*, **29**(8), 1518-1525.
- Ebrahimi, F. and Rastgo, A. (2008), "An analytical study on the free vibration of smart circular thin FGM plate based on classical plate theory", *Thin Walled Struct.*, **46**(12), 1402-1408.
- Efraim, E. and Eisenberger, M. (2007), "Exact vibration analysis of variable thickness thick annular isotropic and FGM plates", *J. Sound Vib.*, **299**(4-5), 720-738.
- Eraslan, A.N. and Akis, T. (2009), "On the plane strain and plane stress solutions of functionally graded rotating solid shaft and solid disk problems", *Acta Mech.*, **181**(1-2), 43-63.
- Genin, G.M. and Birman, V. (2009), "Micromechanics and Structural Response of Functionally Graded, Particulate-Matrix, Fiber-Reinforced Composites", *Int. J. Solids Struct.*, **46**(10), 2136-2150.
- Gupta, U.S., Lal, R. and Jain, S.K. (1990), "Effect of elastic foundation on axisymmetric vibrations of polar orthotropic circular plates of variable thickness", *J. Sound Vib.*, **139**(3), 503-513.
- Gupta, U.S., Lal, R. and Sharma, S. (2006), "Vibration analysis of non-homogeneous circular plate of nonlinear thickness variation by differential quadrature method", *J. Sound Vib.*, **298**(4-5), 892-906.
- Hosseini Hashemi, S., Omid, M. and Rokni Damavandi Taher, H. (2009), "The validity range of CPT and Mindlin plate theory in comparison with 3-D vibration analysis of circular plates on the elastic foundation", *Eur. J. Mech. A Solids*, **28**(3-5), 289-304.
- Hosseini Hashemi, S., Rokni Damavandi Taher, H. and Akhavan, H. (2010), "Vibration analysis of radially FGM sectorial plates of variable thickness on elastic foundations", *Compos. Struct.*, **92**(7), 1734-1743.
- Hosseini Hashemi, S., Rokni Damavandi Taher, H. and Omid, M. (2008), "3-D free vibration analysis of annular plates on Pasternak elastic foundation via p-Ritz method", *J. Sound Vib.*, **311**(3), 1114-1140.
- Hu, G.K. and Weng, G.J. (2000), "The Connections between the double-inclusion model and the Ponte Castaneda- Willis, Mori-Tanaka, and Kuster-Toksoz models", *Mech. Mater.*, **32**(8), 495-503.
- Liew, K.M. and Liu, F.L. (2000), "Differential quadrature method for vibration analysis of shear deformable

- annular sector plates”, *J. Sound Vib.*, **230**(2), 335-356.
- Liew, K.M., Han, J.B., Xiao, Z.M. and Du, H. (1996), “Differential quadrature method for Mindlin plates on Winkler foundation”, *Int. J. Mech. Sci.*, **38**(4), 405-421.
- Liu, F.L. and Liew, K.M. (1999), “Free vibration analysis of Mindlin sector plates numerical solutions by differential quadrature method”, *Comput. Meth. Appl. Mech. Eng.*, **177**(1-2), 77-92.
- Malekzadeh, P. (2009), “Three-dimensional free vibration analysis of thick functionally graded plates on elastic foundations”, *Compos. Struct.*, **89**(3), 367-373.
- Malekzadeh, P. and Karami, G. (2004), “Vibration of non-uniform thick plates on elastic foundation by differential quadrature method”, *Eng. Struct.*, **26**(10), 1473-1482.
- Matsunaga, H. (2000), “Vibration and stability of thick plates on elastic foundations”, *J. Eng. Mech.*, ASCE, **126**(1), 27-34.
- Ming Hung, H. (2010), “Vibration analysis of orthotropic rectangular plates on elastic foundations”, *Compos. Struct.*, **92**(4), 844-852.
- Mori, T. and Tanaka, K. (1973), “Average stress in matrix and average elastic energy of materials with misfitting inclusions”, *Acta Metall.*, **21**(5), 571-574.
- Nie, G.J. and Zhong, Z. (2007), “Semi-analytical solution for three-dimensional vibration of functionally graded circular plates”, *Comput. Mech. Appl.*, **196**(49-52), 4901-4910.
- Nie, G.J. and Zhong, Z. (2010), “Dynamic analysis of multi-directional functionally graded annular plates”, *Appl. Math. Modell.*, **34**(3), 608-616.
- Ponnusamy, P. and Selvamani, R. (2012), “Wave propagation in a generalized thermo elastic plate embedded in elastic medium”, *IMM, An Int. J.*, **5**(1), 13-26.
- Prakash, T. and Ganapathi, M. (2006), “Asymmetric flexural vibration and thermoelastic stability of FGM circular plates using finite element method”, *Compos Part B*, **37**(7-8), 642-649.
- Shafiee, A.A., Daneshmand, F., Askari, E., Mahzoon, M. (2014), “Dynamic behavior of a functionally graded plate resting on Winkler elastic foundation and in contact with fluid”, *Struct. Eng. Mech.*, **50**(1), 53-71.
- Shu, C. (2000), *Differential Quadrature and its Application in Engineering*, Springer, Berlin, Germany.
- Shu, C. and Wang, C.M. (1999), “Treatment of mixed and nonuniform boundary conditions in GDQ vibration analysis of rectangular plates”, *Eng. Struct.*, **21**(2), 125-134.
- Sobhani Aragh, B. and Yas, M.H. (2010), “Static and free vibration analyses of continuously graded fiber-reinforced cylindrical shells using generalized power-law distribution”, *Acta Mech.*, **215**(1-4), 155-173.
- Tahouneh, V. and Yas, M.H. (2012), “3-D free vibration analysis of thick functionally graded annular sector plates on Pasternak elastic foundation via 2-D differential quadrature method”, *Acta Mech.*, **223**(9), 1879-1897.
- Tornabene, F. (2009), “Free vibration analysis of functionally graded conical, cylindrical shell and annular plate structures with a four-parameter power-law distribution”, *Comput. Meth. Appl. Mech. Eng.*, **198**(37-40), 2911-2935.
- Vel, S.S. (2010), “Exact elasticity solution for the vibration of functionally graded anisotropic cylindrical shells”, *Compos. Struct.*, **92**(11), 2712-2727.
- Vel, S.S. and Batra, R.C. (2002), “Exact solution for thermoelastic deformations of functionally graded thick rectangular plates”, *AIAA*, **40**(7), 1421-1433.
- Wang, X. and Wang, Y. (2004), “Free vibration analyses of thin sector plates by the new version of differential quadrature method”, *Comput. Meth. Appl. Mech. Eng.*, **193**(36-38), 3957-3971.
- Xiang, Y., Kitipornchai, S. and Liew, K.M. (1996), “Buckling and vibration of thick laminates on Pasternak foundations”, *J. Eng. Mech.*, ASCE, **122**(1), 54-63.
- Xiang, Y., Wang, C.M. and Kitipornchai, S. (1994), “Exact vibration solution for initially stressed Mindlin plates on Pasternak foundations”, *Int. J. Mech. Sci.*, **36**(4), 311-316.
- Yas, M.H. and Sobhani Aragh, B. (2010), “Free vibration analysis of continuous grading fiber reinforced plates on elastic foundation”, *Int. J. Eng. Sci.*, **48**(12), 1881-1895.
- Zhou, D., Cheung, Y.K., Lo, S.H. and Au, F.T.K. (2004), “Three-dimensional vibration analysis of rectangular thick plates on Pasternak foundation”, *Int. J. Numer. Meth. Eng.*, **59**(10), 1313-1334.

Zhou, D., Lo, S.H., Au, F.T.K. and Cheung, Y.K. (2006), "Three-dimensional free vibration of thick circular plates on Pasternak foundation", *J. Sound Vib.*, **292**(3-5), 726-741.

CC